Dalton Transactions

Accepted Manuscript

ROYAL SOCIETY OF CHEMISTRY

www.rsc.org/dalton

Dalton Transactions

COMMUNICATION

A three-coordinate iron-silylene complex stabilized by ligand-ligand dispersion forces

Received 00th January 20xx,
Accepted 00th January 20xx

DOI: 10.1039/x0xx00000x

www.rsc.org/

Mikko M. Hänninen,[a,b] Kuntal Pal,[a,c] Benjamin M. Day,[a] Thomas Pugh,[a] and Richard A. Layfield*[a]

The structural and bonding properties of a three-coordinate N-heterocyclic silyene (NHSi) complex of the iron(II) amide [Fe{N(SiMe$_3$)$_2$}$_2$] are reported. Computational studies reveal that dispersion forces between the amido SiMe$_3$ substituents and the isopropyl substituents on the NHSi ligand significantly enhance the stabililty of the complex, along with Fe-to-Si π-backbonding.

Low-coordinate carbene complexes of 3d transition metals, especially those containing N-heterocyclic carbenes (NHCs), have attracted considerable interest in recent years. Most efforts have focused on catalytic applications of four-, three- and even two-coordinate metal-carbene complexes; iron has featured prominently in this chemistry as part of the drive towards replacing critically endangered, toxic elements with inexpensive and benign alternatives.[1,2] Carbene ligands have also proven to be adept at stabilizing small-molecule models of important iron-containing biological systems,[3] and they have allowed access to rare or unprecedented iron oxidation states and coordination environments.[4]

Our work in this area has focused on iron-NHC complexes of the type [(NHC)Fe(N′′)$_2$], where the NHC is typically a bulky derivative such as 1,3-di(2,6-diisopropyl)phenylimidazolin-2-ylidene (IPr) and N′′ = N(SiMe$_3$)$_2$. Having examined the electronic structure and bonding in these three-coordinate species,[5] we also ascertained that the NHC ligands often participate in the reactivity of the complex. For example, heating [(IPr)Fe(N′′)$_2$] rearranges the IPr ligand to its abnormal isomer, and similar treatment of [(I^{t}Bu)Fe(N′′)$_2$] eliminates a ^{t}Bu substituent as isobutene (I^{t}Bu = 1,3-bis(*tert*-butyl)imidazole-2-ylidene).[6] Furthermore, a range of [(NHC)Fe(N′′)$_2$] complexes catalyse the reactions of NHCs with primary phosphines, resulting in the formation of carbene-phosphinidenes of the type (NHC)·PR (R = Ph, mesityl).[7]

Whereas low-coordinate iron-carbene complexes are widespread, the analogous chemistry with heavier tetrylenes, such as N-heterocyclic silylene (NHSi) ligands, is still underdeveloped,[8] and 3-coordinate complexes are unknown. This is somewhat surprising in light of the extensive coordination chemistry of silylene ligands with platinum group metals, which has been applied in many elegant catalytic reactions.[9] In light of the rich chemistry of the three-coordinate [(NHC)Fe(N′′)$_2$] complexes, we sought to gain insight into how the different σ- and π-electronic structure of a typical NHSi interacts with a low-coordinate iron(II) centre. We now report our initial findings on the first 3-coordinate iron-silylene complex [(^{Si}IPr)Fe(N′′)$_2$] (**1**, Scheme 1).

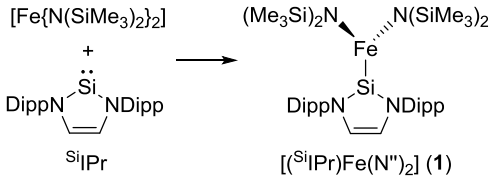

Scheme 1. Synthesis of complex **1** (Dipp = 2,6-diisopropylphenyl).

Complex **1** formed as yellow crystals by recrystallization from toluene at –30°C. Analytically pure samples were obtained by washing the crystals with pentane that had been pre-cooled to –80°C. Typical isolated yields were 20-25% (50-100 mg scale), which reflects the very high solubility of **1** even in cold pentane. X-ray crystallography revealed that the silylene complex crystallizes as **1**·toluene (Fig. 1, Table S1). Molecules of **1** consist of a three-coordinate iron centre bonded to the silicon atom of ^{Si}IPr and to two N′′ ligands. The Fe–Si bond distance is, at 2.496(1) Å, markedly longer than the mean average Fe–Si single bond distance according to the Cambridge Structural Database.[10] It is also noteworthy that the Fe–Si bond in **1** is longer than the Fe–C distance in [(IPr)Fe(N′′)$_2$] by 0.312 Å. The Fe–N bond lengths of 1.941(2) and 1.942(2) Å are very similar to those found in most complexes containing Fe{N(SiMe$_3$)$_2$} units. The N3-Fe1-Si1 and N4-Fe1-Si1 angles are 108.7(1)° and 109.5(1)°, respectively, and the N3-Fe1-N4 angle

[a] School of Chemistry, The University of Manchester, Oxford Road, Manchester, M13 9PL, U.K. E-mail: Richard.Layfield@manchester.ac.uk.
[b] Department of Chemistry, University of Jyväskylä, Jyväskylä, P.O. Box 35, FI-40014, Finland.
[c] Department of Chemistry, University of College of Science, University of Calcutta, 92 A.P.C. Road, Kolkata – 70009, India.
†Electronic Supplementary Information (ESI) available: synthesis, X-ray crystallography, spectroscopy, magnetic measurements, computational details. See DOI: 10.1039/x0xx00000x

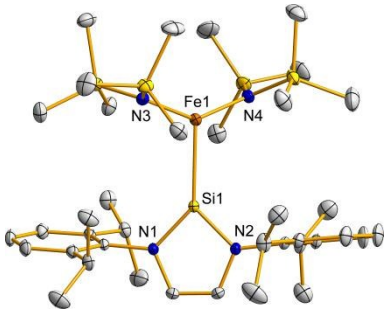

Fig. 1 Molecular structure of **1**, with 30% thermal ellipsoids. Hydrogen atoms are omitted. Unlabelled atoms are silicon (yellow) and carbon (grey).

is 141.81(8)°.

The magnetic susceptibility of **1**·toluene was measured in the temperature range 2-300 K (Fig. 2). The value of $\chi_M T$ at 300 K is 3.70 cm^3 K mol^{-1}, with very little variation down to approximately 60 K. At lower temperatures, $\chi_M T$ decreases gradually before experiencing a precipitous drop below 10 K due to zero-field splitting (ZFS) effects; a value of 1.95 cm^3 K mol^{-1} is reached at 2 K. The field (*H*) dependence of the magnetization (*M*) was measured at 1.8 K and 3.0 K, with both sets of data showing a steep increase in magnetization as the field increases to approximately 10 kOe (Fig. 2). In stronger fields the magnetization increases more slowly, without quite reaching saturation, to become 2.56 μ_B and 2.53 μ_B at 7 T and 1.8 K and 3.0 K, respectively. The susceptibility and magnetization data were both fitted accurately using PHI[11] with $S = 2$, $g_{x,y} = 2.14$, $g_z = 2.32$, and a ZFS parameter of $D = -22.6$ cm^{-1}.† These parameters are similar to those determined for other three-coordinate Fe(II) complexes.[5,12]

The ^{1}H NMR spectrum of **1**·toluene in toluene-D_8 at 298 K (Figs 3, S1) is remarkable for the absence of paramagnetically shifted ^{Si}IPr resonances, which would be expected if the silylene ligands were coordinated to a high-spin iron(II) centre. Indeed, the NMR spectrum clearly shows a series of resonances in the range $\delta(^1H)$ = 0-9 ppm, all of which can be assigned to the distinct environments of free ^{Si}IPr. Thus, the isopropyl methyl protons occur at 0.72 and 1.89 ppm, and the associated methine protons occur as a broad resonance at 1.51 ppm. The Dipp aromatic protons resonate in the range 7.26-7.37 ppm, and the silylene backbone protons occur as a broad singlet at 8.77 ppm. The only other significant resonance

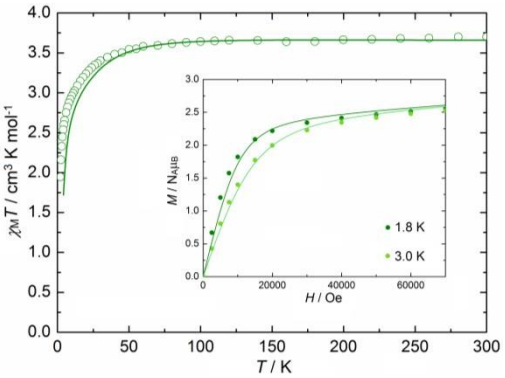

Fig. 2 $\chi_M T$ vs *T* for **1**·toluene in an applied field 10 kOe. Inset: *M* vs. *H* at 1.8 K and 3.0 K. For both graphs, the solid lines represent fits to the data using the parameters stated in the text.

in the ^{1}H NMR spectrum at 298 K occurs at 60.70 ppm, which is close to the value reported for the $SiMe_3$ protons in $[Fe(N'')_2]$ itself.[12] These observations indicate that the ^{Si}IPr ligand is either dissociated from the iron centre at 298 K, or that a dynamic process occurs in which the NHSi coordinates and dissociates at a faster rate than the experiment timescale.

To investigate this further, the ^{1}H NMR spectrum of **1**·toluene was studied in the temperature range 238-328 K at intervals of 10 K. A selection of the spectra is shown in Fig. 3, with the full set provided in the ESI (Fig. S3). All the resonances broaden upon cooling, and the resonances due to the isopropyl methyl substituents shift appreciably to higher fields. The resonance due to the $SiMe_3$ groups of $[Fe(N'')_2]$ broadens significantly upon cooling. The VT-NMR spectra suggest that the ^{Si}IPr ligand does indeed coordinate to iron in solution, but also that it is extremely labile.

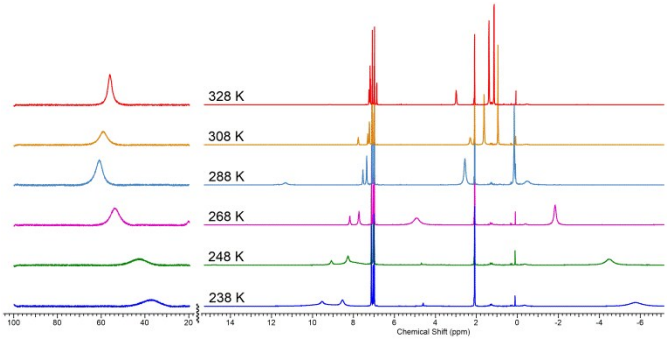

Fig. 3 Variable-temperature (238-328 K) ^{1}H NMR spectrum of **1**·toluene in toluene-D_8.

To gain further insight into the structure and bonding in **1**, we have performed a thorough computational analysis using density functional theory (DFT). In addition to probing the nature of the Fe–Si interaction in **1**, we were also interested in the role of other intramolecular interactions that could contribute to the (in)stability of the complex. In particular, interactions between the $SiMe_3$ and ^{i}Pr substituents are of interest. The structure of **1** presents a picture dominated by steric bulk and hence repulsive interactions between the ^{Si}IPr ligand and the *bis*(trimethylsilyl)amido ligands. However, recent computational studies on low-coordinate main group and transition metal compounds have re-evaluated the way in which bulky substituents influence stability.[14-16] A consistent picture has emerged in which the stability of many low-coordinate species is due largely to the attractive dispersion forces between the CH groups within alkyl or silyl substituents. Here, steric bulk is advantageous because it allows the CH groups of one ligand to extend into sufficiently close proximity to the CH groups of another ligand, and so to engage in 'steric attraction'.[17] Complex **1** is clearly a system in which dispersion forces could be important, hence calculations of such interactions formed an important part of our study.

All calculations were performed using Turbomole[18] or ADF[19] program packages. The geometry of **1** was optimized using the PBE1PBE functional with the Def2-TZVP basis set for the iron atom and the silicon atom of the ^{Si}IPr ligand, and the Def2-SVP basis set was used for all other atoms. This

combination of basis sets is referred to as Def2-mix. A full geometry optimization for **1** was also carried out using the Def2-TZVP basis set for all atoms, and the resulting geometrical parameters were similar to those obtained using Def2-mix. Thus, for computational efficiency, the Def2-mix basis set was used for all subsequent calculations. The calculations were run with and without corrections for dispersion effects, with the former being accomplished using Grimme's DFT-D3 method.[20,21]

The geometry of **1** optimized at the DFT-D3 level is in excellent agreement with the crystallographically determined structure, with only small discrepancies between calculation and experiment (Table 1). The calculated Fe–Si distance is underestimated merely by 0.0054 Å, and the Fe–N distances are underestimated by 0.008 Å. The impact of the inter-ligand CH···HC dispersion forces becomes apparent when comparing the optimized geometry without the dispersion correction (DFT level) to the experimental and DFT-D3 structures. Whereas most of the bond lengths and angles are reproduced accurately by the DFT level calculations, the Fe–Si bond length is overestimated by 0.0532 Å relative to the experimental structure, which is almost ten times greater than the discrepancy at the DFT-D3 level.

Further insight into the dispersion interactions was obtained using wave-function-based approaches, namely (unrestricted) Hartree-Fock (HF) and second-order Møller-Plesset perturbation theory (MP2). As electron correlation is neglected by the HF method, dispersion effects are essentially excluded from the calculation. In contrast, MP2 considers closed-shell interactions. Thus, comparing the two methods provides insight into the effects of dispersion forces within molecules of **1**. Whereas the MP2 geometry optimization produced an excellent agreement with experiment, the agreement obtained using HF methods is poor. In particular, the Fe–Si bond is massively overestimated by 0.5124 Å in the HF calculation, whereas the MP2 calculation produces an extremely small discrepancy of 0.0008 Å. These results strongly support the claim that structure of **1** experiences significant stabilization from dispersion forces.

Table 1. Key bond lengths [Å] and angles [°] in the experimental and calculated structures of **1**.

	expt.	DFT-D3	DFT	HF	MP2
Fe1–Si1	2.4957(7)	2.4903	2.5489	3.0081	2.4949
Fe1–N3	1.941(2)	1.934	1.943	2.027	1.955
Fe1–N4	1.942(2)	1.934	1.943	2.027	1.955
Si1–N1	1.727(2)	1.740	1.745	1.722	1.739
Si1–N2	1.727(2)	1.740	1.745	1.722	1.739
N3-Fe1-N4	141.81(8)	143.73	141.49	143.9	143.34
N3-Fe1-Si1	108.7(1)	108.2	109.4	108.0	108.3
N4-Fe1-Si1	109.5(1)	108.1	109.1	108.1	108.4
N1-Si1-N3	89.3(1)	88.8	88.9	90.1	88.6

Table 2. Energy decomposition analysis for **1** (in units of kcal mol^{-1}).[a]

	ΔE_{int}	ΔE_{elstat}	ΔE_{Pauli}	ΔE_{orb}	ΔE_{disp}	steric
DFT	–42.6	–62.9	73.5	–53.2		18.0
DFT-D3	–63.6	–77.3	95.3	–58.8	–22.7	10.6

$\Delta E_{int} = \Delta E_{elstat} + \Delta E_{Pauli} + \Delta E_{orb} + \Delta E_{disp}$; steric = $\Delta E_{elstat} + \Delta E_{Pauli}$.

The bonding in **1** was interrogated further using an energy decomposition analysis (EDA).[22] The (instantaneous) interaction energy, ΔE_{int}, is the energy change associated with combining the ^{Si}IPr and [Fe(N′′)$_2$] fragments to give **1**. ΔE_{int} is analysed by decomposing the total interaction into a sum of electrostatic interactions (ΔE_{elstat}), Pauli repulsion (ΔE_{Pauli}) and orbital interactions (ΔE_{orb}). The EDA was conducted for **1** with and without dispersion forces (Table 2).

In both sets of calculations, the orbital interaction term makes a significant contribution to ΔE_{int}, which is not unexpected for the NHSi ligand in light of its charge-neutral nature. The attractive electrostatic terms are outweighed by the Pauli repulsion, resulting in small but significant steric repulsions (steric = ΔE_{elstat} + ΔE_{Pauli}). Although the overall interaction energy in the case of **1** without dispersion forces is an appreciable –42.6 kcal mol^{-1}, including dispersion forces significantly enhances ΔE_{int} to –63.6 kcal mol^{-1}, i.e. ΔE_{disp} provides about one-third of the total attractive interaction.

The Fe–Si orbital interaction in **1** was further probed using the extended transition-state natural orbitals for chemical valence (ETS-NOCV) method.[23] This approach can be used to partition ΔE_{orb} into σ- and π-contributions, thus allowing the donation of electron density from ligand to metal, and from metal to ligand, to be studied. Inspection of the NOCV deformation densities $\Delta\rho$ (Fig. 4) shows that the largest contribution to the Fe–Si bond is silicon-to-iron σ-donation (–19.5 kcal mol^{-1}), however three π-type iron-to-silicon back-bonding interactions account for –25.2 kcal mol^{-1}.

Finally, the Fe–Si bond dissociation energy (BDE) of **1** was calculated with (DFT-D3 level) and without (DFT level) the effects of dispersion forces. At the DFT-D3 level, the BDE for **1** is 31.1 kcal mol^{-1}, and at the DFT level the BDE is 8.1 kcal mol^{-}

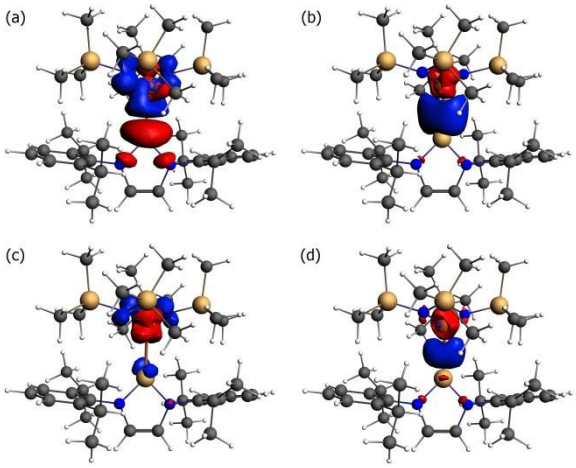

Fig. 4 The four largest NOCV deformation densities ($\Delta\rho$) contributions (–44.7 kcal mol^{-1}) in **1** (red $\Delta\rho < 0$; blue $\Delta\rho > 0$). (a) Si-to-Fe σ-donation. (b) Fe-to-Si π-donation. (c) Fe-to-Si π-donation. (d) Fe-to-Si π-donation.

[1]. Thus, dispersion forces strengthen the interaction of the ^{Si}IPr ligand with the Fe(N'')$_2$ unit in **1** by a factor of almost four, which further highlights the importance of intramolecular ligand-ligand interactions in stabilizing the complex.

To conclude, [(^{Si}IPr)Fe(N'')$_2$] (**1**) is the first 3-coordinate iron NHSi complex. An S = 2 ground state was found for **1**, along with a large negative axial ZFS parameter of D = –22.6 cm^{-1}. A computational study of **1** revealed that dispersion forces play a significant role in stabilizing the interaction with the ^{Si}IPr ligand, although these inter-ligand attractive interactions are readily overcome in solution, as witnessed by the lability of the ^{Si}IPr ligand in toluene at room temperature. The nature of the Fe–Si bond was also studied computationally, and found to consist of a silicon-to-metal σ-donor interaction supported by appreciable iron-to-silicon π-back-bonding.

Our observations imply that NHSi ligands should be particularly effective at stabilizing low-valent, low-coordinate iron centres, which could conceivably feed into the design of NHSi-containing iron catalysts. More generally, our results support the notion that NHSi ligands are not simply heavier analogues of NHCs, and that NHSi ligands should have considerable potential for applications in low-coordinate transition metal chemistry.

Notes and references

The authors thank The Academy of Finland (Research Fellowship to MM) and the EPSRC (EP/K039547/1) for funding.

1 M. J. Ingleson and R. A. Layfield, *Chem. Commun*. 2012, **48**, 3579.
2 (a) J. A. Przyojski, K. P. Veggenberg, H. D. Arman and Z. J. Tonzetich, *ACS Catalysis*, 2015, **5**, 5938. (b) K. Riener, S. Haslinger, A. Raba, M. P. Högerl, P. Cokoja, W. A. Hermann and F. Kühn, *Chem. Rev*., 2014, **114**, 5215.
3 R. Pulukkody and M. Y. Darensbourg, *Acc. Chem. Res*., 2015, **48**, 2049.
4 (a) G. E. Cutsail III, B. W. Stein, D. Subedi, J. M. Smith, M. L. Kirk and B. M. Hoffmann, *J. Am. Chem. Soc*., 2014, **136**, 12323. (b) J. J. Scepaniak, C. S. Vogel, M. M. Khusniyarov, F. W. Heinemann, K. Meyer and J. M. Smith, *Science*, 2011, **331**, 1049.
5 R. A. Layfield, J. J. W. McDouall, M. Scheer, C. Schwarzmaier and F. Tuna, *Chem. Commun*. 2011, **47**, 10623.
6 (a) B. M. Day, T. Pugh, D. Hendriks, C. Fonseca Guerra, D. J. Evans, F. M. Bickelhaupt and R. A. Layfield, *J. Am. Chem. Soc*. 2013, **135**, 13338. (b) T. Pugh and R. A. Layfield, *Dalton Trans*., 2014, **43**, 4251.
7 K. Pal, O. B. Hemming, B. M. Day, T. Pugh, D. J. Evans and R. A. Layfield, *Angew. Chem. Int. Ed*., 2016, **55**, 1690.
8 (a) Thomas A. Schmedake, M. Haaf, B. J. Paradise, A. J. Millevolte, D. R. Powell and R. West, *J. Organomet. Chem*., 2001, **636**, 17. (b) N. C. Breit, C. Eisenhut and S. Inoue, *Chem. Commun*., 2016, DOI: 10.1039/c6cc00601a.
9 a) B. Blom, M. Stoelzel and M. Driess, *Chem. Eur. J*., 2013, 19, 40. (b) B. Blom, D. Gallego and M. Driess, *Inorg. Chem. Front*., 2014, **1**, 134. (c) D. Gallego, S. Inoue, B. Blom, M. Driess, *Organometallics*, 2014, **33**, 6885.
10 Mercury 3.8, accessed 20/06/2016, Copyright Cambridge Crystallographic Data Centre, 2001-2016. http://www.ccdc.cam.ac.uk/mercury/
11 N. F. Chilton, R. P. Anderson, L. D. Turner, A. Soncini and K. S. Murray, *J. Comput. Chem*., 2013, **34**, 1164.
12 S. A. Sulway, D. Collison, J. J. W. McDouall, F. Tuna and R. A. Layfield, *Inorg. Chem*., 2011, **50**, 2521.
13 (a) M. M. Olmstead, P. P. Power and S. C. Shoner, *Inorg. Chem.*, 1991, **30**, 2547.
14 (a) J. –D. Guo, D. J. Liptrot, S. Nagase and P. P. Power, *Chem. Sci*., 2015, **6**, 6235. (b) M. Faust, A. M. Bryan, A. Mansikkamäki, P. Vasko, M. M. Olmstead, H. M. Tuononen, F. Grandejean, G. J. Long and P. P. Power, *Angew. Chem. Int. Ed*., 2015, **54**, 12914. (c) C. –Y. Lin, J. –D. Guo, J. C. Fettinger, S. Nagase, F. Grandjean, G. J. Long, N. F. Chilton and P. P. Power, *Inorg. Chem*., 2013, **52**, 13584. (d) B. D. Rekken, T. M. Brown, J. C. Fettinger, F. Lips, H. M. Tuononen, R. H. Herber and P. P. Power, *J. Am. Chem. Soc*., 2013, **135**, 10134. (e) J. –D. Guo, S. Nagase and P. P. Power, *Organometallics*, 2015, **34**, 2028.
15 (a) S. Grimme and P. R. Schreiner, *Angew. Chem. Int. Ed*., 2011, **50**, 12639.
16 (a) N. Sieffert and M. Buehl, *Inorg. Chem*., 2009, **48**, 4622. (b) A. A. Fokin, L. V. Chernish, P. A. Gunchenko, E. Y. Tikhonchuk, H. Hausmann, M. Serafin, J. E. P. Dahl, R. M. K. Carlson and P. R. Schreiner, *J. Am. Chem. Soc*., 2012, **134**, 13641. (c) H. Arp, J. Baumgartner, C. Marschner, P. Zark and T. Müller, *J. Am. Chem. Soc*., 2012, **134**, 6409. (d) P. R. Schreiner, L. V. Chernish, P. A. Gunchenko, E. Y. Tikhonchuk, H. Hausmann, M. Serafin, S. Schlecht, J. E. P. Dahl, R. M. K. Carlson and A. A. Fokin, *Nature*, 2011, **477**, 308.
17 L. P. Wolters, R. Koekkoek, F. M. Bickelhaupt, *ACS Catalysis*, 2015, **5,** 5766.
18 TURBOMOLE V6.6 2014, a development of University of Karlsruhe and Forschungszentrum Karlsruhe GmbH, 1989-2007, TURBOMOLE GmbH, since 2007; available from http://www.turbomole.com
19 ADF2014, SCM, Theoretical Chemistry, Vrije Universiteit, Amsterdam, The Netherlands, http://www.scm.com
20 (a) S. Grimme, J. Antony, S. Ehrlich and H. Krieg, *J. Chem. Phys*., 2010, **13**2, 154104. (b) S. Grimme, S. Ehrlich and L. Goerigk, *J. Comput. Chem*., 2011, **32**, 1456.
21 M. Nishio, *Phys. Chem. Chem. Phys*., 2011, **13**, 13873.
22 T. Ziegler and A. Rauk, *Theor. Chim. Acta*, 1977, **46**, 1.
23 M. P. Mitoraj, A. Michalak and T. Ziegler, *J. Chem. Theory Comput*., 2009, **5**, 962.